

Diffusion weighted imaging and apparent diffusion coefficient discrimination of odontogenic keratocyst

Antonione Santos Bezerra
Pinto ¹
André Luca Araújo de Sousa²
Carlos Alberto Monteiro
Falcão ²
Maria Ângela Arêa Leão
Ferraz ²
João Pedro Perez Gomes ³
Sérgio Lúcio P. de Castro
Lopes ⁴
Paulo Henrique Braz da Silva ³
André Luiz Ferreira Costa ⁵
Luana Leal Cosmo Cardoso ^{2*} 

Abstract:

Radiological diagnosis of Odontogenic Keratocyst (OKC) is particularly challenging due to its radiological similarities in comparison to other odontogenic lesions. This study aimed to provide data from the literature review and to present a case report in which the diffusion-weighted imaging (DWI) and the apparent diffusion coefficient (ADC) using magnetic resonance imaging (MRI) were obtained to establish a possible way to differentiate OKC from other odontogenic lesions. Literature review data and its association with the present case report shows the potential to use DWI and ADC combination as a possible tool to differentiate OKC from ameloblastomas.

Keywords: Odontogenic Cysts, Magnetic Resonance Imaging, Diffusion Weighted Imaging.

¹ Instituto de Educação Superior do Vale do Parnaíba (IESVAP), - Parnaíba - Piauí - Brasil.

² Universidade Estadual do Piauí (UESPI), - Parnaíba - Piauí - Brasil.

³ Universidade de São Paulo (USP), Department of Stomatology, Division of General Pathology, School of Dentistry - São Paulo - São Paulo - Brasil.

⁴ Universidade Estadual Paulista Júlio de Mesquita Filho-ICT UNESP, Postgraduate Program in Oral Biopathology-Institute of Science and Technology - São José dos Campos - São Paulo - Brasil.

⁵ Universidade Cruzeiro do Sul, Postgraduate Program in Dentistry - São Paulo - São Paulo - Brasil.

Correspondence to:

Luana Leal Cosmo Cardoso.
E-mail: luanalccardoso@outlook.com

Article received on July 23, 2023.

Article accepted on August 21, 2023.

DOI: 10.5935/2525-5711.20230230



INTRODUCTION

Odontogenic keratocyst (OKC), first described by in 1956 by Philipsen, is a benign intraosseous lesion of odontogenic origin, accounting for approximately 10% of all mandibular cysts.

OKCs classification can be considered controversial since in the 4th edition of the World Health Organization (WHO) Classification of Head and Neck Tumors, the previous classification of keratocystic odontogenic tumors (KCOT) has been reclassified to OKC¹.

Symptoms comprise swelling, pain, and sinus tract formation², but it can also present as an asymptomatic entity³, despite its described local aggressiveness.

Recurrence rates have been reported in up to 14% of the cases⁴, and in 25% in some studies³.

Radiological diagnosis is particularly challenging, with authors highlighting that only 28% of OKC has shown typical radiographic features, such as multilocular appearance, and the only reliable radiographic parameter described is the lack of cortical expansion in most OKCs in comparison with other odontogenic lesions, such as ameloblastomas and other odontogenic cysts, tending to hollow the mandible and fenestrate the lingual cortex³.

This study aimed to describe an OKC case with the assessment of diffusion-weighted imaging (DWI) and the apparent diffusion coefficient (ADC) using magnetic resonance imaging (MRI) and to compare the obtained values to the ones previously presented in the medical literature. Besides, we also provide data regarding volume analysis.

CASE HISTORY

An 18 years old female patient sought dental care for evaluation by imaging exams for orthodontic purposes. Panoramic radiography (PR) and a lateral teleradiography (LT) were performed (Figure 1). After analysis of the imaging exams, an extensive radiolucent lesion was detected in the left mandibular region. A Cone-Beam Computed Tomography (CBCT) was then performed and, for a case study, the use of DWI and ADC to the Magnetic Resonance (MR) protocol. For the imaging study to be possible, all ethical parameters were followed, with patient signing the free and informed consent term.

The use of three-dimensional methods is essential to analyze the morphology and topography of the lesion, contributing to a safer treatment. The volume of OKC was calculated with the aid of computer software

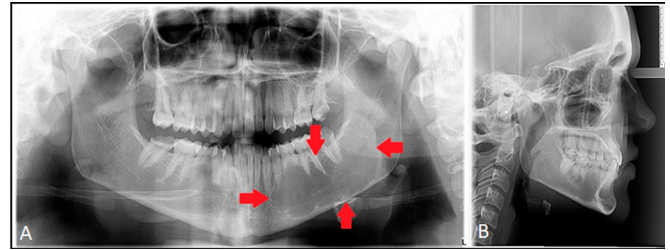


Figure 1 A. Panoramic radiography showing radiolucent lesion in the left mandibular region. B. Lateral teleradiography.

(InVesalius[®] 3.1 version – cti.gov.br/invesalius) through manual segmentation technique (Figure 2)^{5,7}. The lesion measured 8392.289 mm³ (Figure 3).

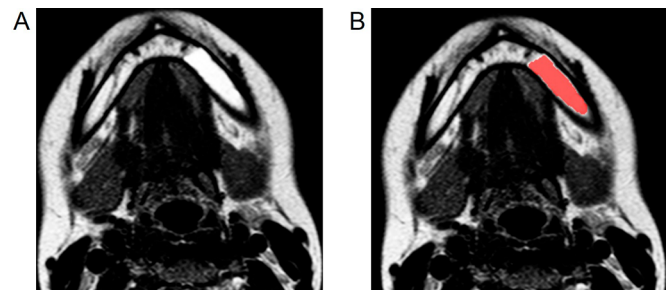


Figure 2 A. Axial slice of weighted T2 magnetic resonance image showing a hypersignal structure on the left side of mandible. B. Manual segmentation process for further three-dimensional reconstruction and volume calculation.

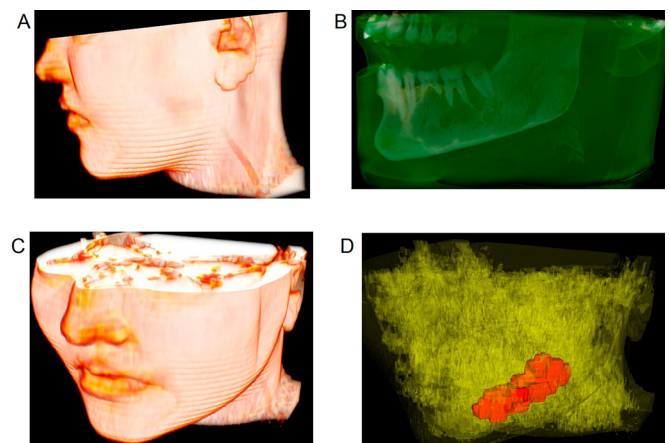


Figure 3 A. Magnetic resonance imaging (MRI) reconstruction of the skull in lateral perspective. B. Cone beam computed tomography reconstruction of the lesioned mandible. C. MRI reconstruction of the skull in isometric perspective. D. Three-dimensional volume reconstruction of the lesion in isometric perspective with altered skull transparency and colour.

IMAGING ASSESSMENT

PR analysis showed an extensive unilocular radiolucent lesion in the region of the body, angle and left mandibular branch, with an aspect of anteroposterior

growth, in addition to having irregular and sclerotic borders and root resorption of the teeth referring to the lesion area. (Figure 1A).

There was an evaluation focusing on coronal, axial and sagittal slices with further volumetric reconstruction with the aid of computer software (InVesalius® 3.1 version - <https://www.cti.gov.br/pt-br/invesalius>). A CBCT scan was performed using GXCB-500TM powered by i-CAT® with 16x6 cm FOV, yielding slice thickness and reconstruction interval of 0.2 mm each. Subsequently, parasagittal images were obtained with a 1 mm slice thickness. The presence of a hypodense osteolytic structure was assessed, located in the cortical area in the left mandibular body, extending from the tooth 33 to 38 in the anteroposterior direction. In the inferior-superior direction, the lesion extends from mandibular base until the roots of teeth 34, 75, 36 and 37.

Growth is observed in the medullary bone region in the anteroposterior direction with the involvement of the base of the mandible without the presence of bone expansion, areas of severe thinning and compromised mandibular canal (Figure 2). The CBCT study suggested as a diagnostic hypothesis OKC or ameloblastoma. Histopathological examination confirmed OKC diagnosis, a cystic space containing desquamated keratin lined with a parakeratinised squamous epithelium. OKC measures are described in Table 1.

MRI AND DWI

MRI was performed using a 1.5 Tesla scanner (Sigma General Electric, Milwaukee, USA) with a skull coil for axial, coronal and sagittal planes. T1 and T2 weighted images were obtained with an 8-channel skull coil, T1 (RT = 478 ms, isotropic voxel size of 0.72 mm, ET = 16 ms, 1.0 x 21 FOV, 0 cm, slice interval = 2.0 mm) and T2 sequences (RT = 6.5 ms, voxel isotropic size of 0.72 mm, ET = 90.0 ms, FOV of 21.0 x 21.0 cm, slice interval = 2.0 mm).

T1 and T2 weighted images, were performed to assess the actual limits of the lesion and its relationship with the surrounding structures to plan a proper treatment approach (Figure 4). T1 images revealed an intermediate signal in the entire left body

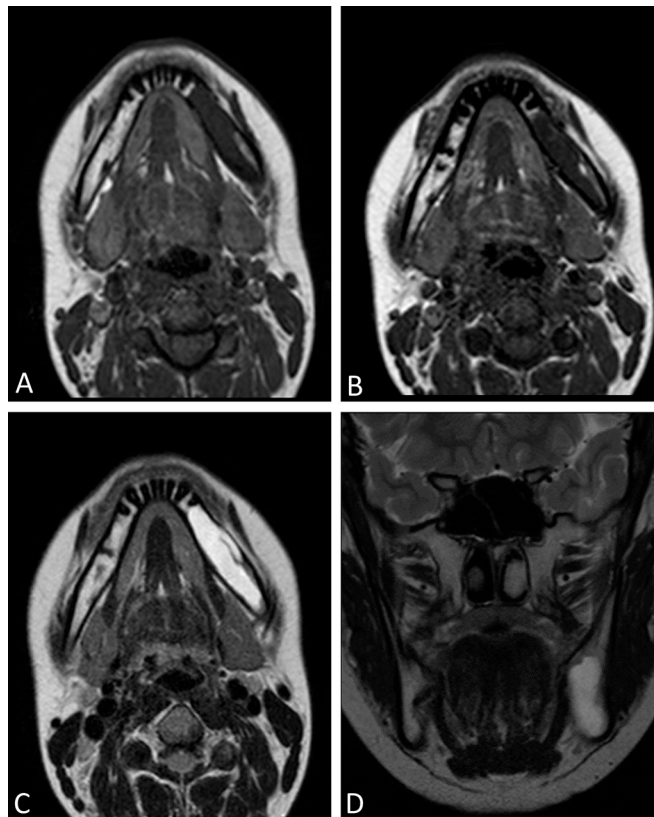


Figure 4. A. and B. T1 weighted axial slices. C. T2 weighted axial slice. D. T2 weighted coronal slice.

of the mandible, without rupture of the lingual and vestibular cortical bone. It was possible to observe well-defined boundaries of the lesion without muscle invasion. T2 images showed the same aspects as T1 images with evidence of hypersignal.

In addition to T1 and T2 weighted sequences, the DWI was performed using the same 1.5 T coil with axial diffusion using the single spin-echo technique and with a b-factor of 0 and 800 s / mm² (Figure 5). The parameters were: TR = 2500 to 3000 ms, TE = 70 ms, matrix 128 x128, section thickness of 5 mm, with intersection interval of 0.5 mm, FOV equal to 24 cm and 8 acquisitions¹⁶. Thus, generating the ACD value map by restricted diffusion. ACD values were measured for normal structures in the upper neck area and for cystic lesions in the mandible. The ADC value was presented as mean + standard deviation (A x 10⁻³ mm² / s), obtaining a lesion value in study of 1.07 ± 0.30 × 10⁻³ mm²/s

Table 1. Odontogenic keratocyst measures.

Region	Length (mm)	Width (mm)	Thickness (mm)
Posterior left side of mandible	22,56	59,46	12,90

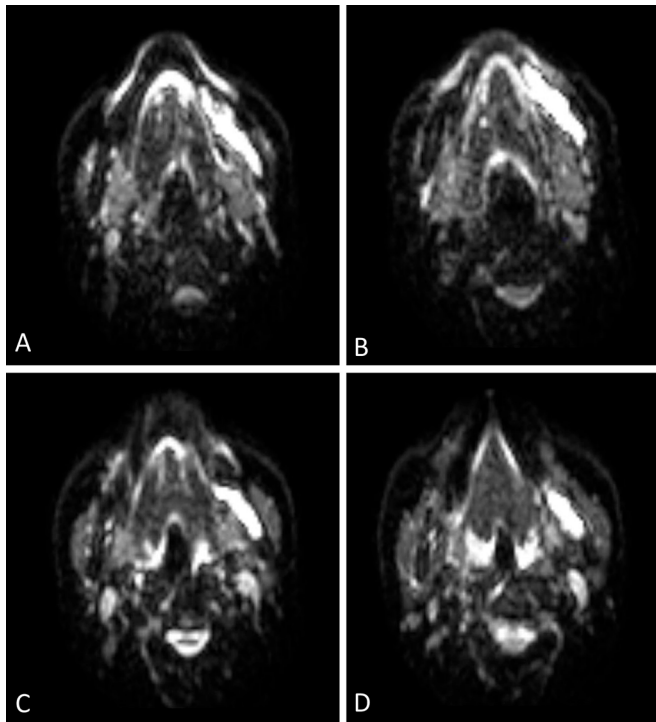


Figure 5. Examples of MRI diffusion weighted images (DWI) axial slices.

DISCUSSION

Odontogenic keratocyst (OKC), first described by in 1956 by Philipsen, is a benign intraosseous lesion of odontogenic origin, accounting for approximately 10% of all mandibular cysts (table 2).

Table 2. Summary of investigations selected according to Author / year of publication, strength of the magnet in Tesla (T) and type of article published.

Author/Year	TESLA	Type of study
Sumi <i>et al.</i> (2008)	1,5 T	Research article
Casseta <i>et al.</i> (2012)	3 T	Retrospective Research
Srinivasan <i>et al.</i> (2012)	1,5 T	Research article
Serifoglu <i>et al.</i> (2015)	1,5 T	Research article
Sakamoto <i>et al.</i> (2016)	3 T	Research article
Oda <i>et al.</i> (2017)	1,5 T	Research article
Han <i>et al.</i> (2018)	1,5 T	Research article
Ogura <i>et al.</i> (2019)	1,5 T	Research article
Vanagundi <i>et al.</i> (2020)	3 T	Research article

OKCs classification can be considered controversial since in the 4th edition of the World Health Organization (WHO) Classification of Head and Neck Tumors, the previous classification of keratocystic odontogenic tumors (KCOT) has been reclassified to OKC¹.

Symptoms comprise swelling, pain, and sinus tract formation², but it can also present as an asymptomatic entity³, despite its described local aggressiveness.

Recurrence rates have been reported in up to 14% of the cases⁴, and in 25% in some studies³.

Radiological diagnosis is particularly challenging, with authors highlighting that only 28% of OKC has shown typical radiographic features, such as multilocular appearance, and the only reliable radiographic parameter described is the lack of cortical expansion in most OKCs in comparison with other odontogenic lesions, such as ameloblastomas and other odontogenic cysts, tending to hollow the mandible and fenestrate the lingual cortex³.

Although OKCs are described as benign intraosseous lesions, they are known to present an aggressive behavior with a high recurrence rate and mitotic activity superior to other dental cysts. In addition to its particular behavior, there is the fact that the lesion is associated with a mutation or inactivation of tumor suppressor genes¹.

The diagnosis of lesions in the head and neck region is difficult due to the anatomical and histological components of the different tissues^{8,10}. Regarding OKC, the use of different imaging modalities combined is important not only for the diagnosis, but also for the differentiating OKC from other odontogenic lesions, since OKC treatment is variable considering it may require a more invasive approach, depending on its aggressiveness, than other lesions with similar radiological characteristics.

DWI is a short sequence produced from echo-planar imaging (EPI), fast advanced spin echo (FASE) and split-echo acquisition (SPLICE)^{8,9,11}. In the present case, a 1.5 Tesla scanner was used for the strength of the magnet, similar to other studies (Table 3), with axial diffusion using eco-planar technique with single shot spin-echo and with b-factor of 0 and 800 s/mm².

From DWI, it is possible to generate maps with ADC to provide a quantitative index of water diffusivity in each voxel, considering the sensitivity to physiological parameters such as vascularization, cellularity, cytoplasmic nucleus, the integrity of tissue membranes, pressure and viscosity, from Brownian movements of H₂O micro-molecules without the use of radiation or contrast agents to provide functional information. In recent years, it has proven a good biomarker tool for differentiating benign and malignant masses, in addition to assessing normal tissue^{8,9,11,12,13,14,15}.

According to several authors, maps generated from ADC were useful to assist in the diagnostic process, since it may contribute to differentiate OKC from

Table 3. Summary of investigations selected according to results of ADC values of odontogenic lesions.

Author/Year	Odontogenic Lesion	ADC (x 10 ⁻³ mm ² /s)
SUMI <i>et al.</i> (2008)	Odontogenic Keratocyst	1.13 + 0.56
	Ameloblastoma	1.39 + 0.16
SRINIVASAN <i>et al.</i> (2012)	Ameloblastoma (solida areas)	1.041 + 0.41
	Ameloblastoma (cytic areas)	2.192 + 0.33
	Odontogenic Keratocyst	1.019 + 0.07
	Odontogenic Myxoma	2.091 + 0.19
SAKAMOTO <i>et al.</i> (2016)	Dentigerous Cyst	1.23 + 0.09
	Odontogenic Cysts	1.31 + 0.593
	Odontogenic Keratocyst	0.926 + 0.204
ODA <i>et al.</i> (2018)	Ameloblastomas	2.45 + 0.053
	Odontogenic Keratocyst	0.85 + 0.20
HAN <i>et al.</i> (2018)	Unicystic Ameloblastoma	2.309 + 0.17
	Multicystic Ameloblastoma (cystic / solid areas)	1.936 + 0.29 / 1.363 + 0.20
	Odontogenic Keratocyst	0.923 + 0.20
OGURA <i>et al.</i> (2019)	Dentigerous Cyst	1.257 + 0.05
	Odontogenic Keratocyst	1.03 + 0.31
	Radicular Cyst	1.82 + 0.71
VANAGUNDI <i>et al.</i> (2020)	Dentigerous Cyst	1.67 + 1.06
	Unicystic Ameloblastoma	2.518
	Odontogenic Keratocyst	2.217
	Dentigerous Cyst	2.150

other lesions with similar radiological features, including odontogenic myxomas (OM), dentigerous cysts (DC) and, mainly, unicystic ameloblastomas^{8,14,15,16,17}. According to Sumi *et al.* (2008),¹⁵ Han *et al.* (2018)¹⁶ and Borghesi *et al.* (2018)¹, the cystic components of unicystic ameloblastomas have shown a free diffusion and high ADC values, which may be justified by the necrotic content with less viscosity, in addition to slightly protein liquid. In contrast, odontogenic cysts showed restricted diffusion and low ADC values, possibly due to the high viscosity of its content (glycosaminoglycans and hyaluronic acid) and the presence of flaking keratin. Other studies have reported similar ADC values, justifying the differentiation of ameloblastomas from other odontogenic cysts in the literature and the present case (Table 4).

However, concerning ameloblastomas composed of more solid areas, there is restricted diffusion and low ADC values, which can be explained by the high tumor cellness and a higher nucleus-proportion of cytoplasm¹⁴. In the parameters obtained by Ogura *et al.* (2019)⁸, the mean ADC value of the five odontogenic keratocysts ($1.03 \pm 0.31 \times 10^{-3} \text{ mm}^2/\text{s}$) was lower than one simple bone cyst ($2.79 \times 10^{-3} \text{ mm}^2/\text{s}$), three nasopalatine duct cysts ($2.28 \pm 0.12 \times 10^{-3} \text{ mm}^2/\text{s}$), three radicular cysts ($1.82 \pm 0.71 \times 10^{-3} \text{ mm}^2/\text{s}$) and four dentigerous cysts ($1.67 \pm 1.06 \times 10^{-3} \text{ mm}^2/\text{s}$), suggesting the usefulness of DWI in odontogenic keratocysts, especially ADC maps

Table 4. Summary table of the Keratocyst.

Etiology	There is a consensus in the literature that the keratocyst arises from the cellular remains of the dental lamina.
Incidence	Most studies indicate an incidence of 3% to 11% of all odontogenic cysts. But there are also several reports of distinct frequencies documented.
Gender ratio	There is a slight prevalence in males.
Age predilection	They can be found at different ages, but about 60% are found between the ages of 10 to 40 years old.
Risk factors	Its growth may be related to genetic factors inherent in its own epithelium or to enzymatic activity in the fibrous wall of the cyst.
Treatment	Enucleation and curettage. Many surgeons recommend a peripheral ostectomy of the bone cavity to reduce the chance of recurrence. Cauterization of the cavity with Carnoy's solution
Prognosis	Despite a tendency to relapse, the prognosis is considered good.

Source: Neville *et al.* (2016).

for the characterization of normal structures and cystic lesions in the jaw. However, it is important to highlight that the ADC maps comparison may present limitations that can influence in the final result, such as the magnet strength (table 3) and parameters acquisition. In the present clinical case report, the ADC value ($1.07 \pm 0.30 \times 10^{-3} \text{ mm}^2/\text{s}$) was inferior in comparison to values of other lesions found in the literature (Table 4).

Although odontogenic myxoma (OM) has a predilection for the maxilla instead of the mandible and has some developed internal bone trabeculae that differentiate it from other lesions of dental origin, Srinivasan et al. (2012)¹⁴ demonstrated free diffusion and high ADC values in relation to the myxoma, which can be justified by the existence of a myxoid matrix with abundant free water in the extracellular spaces. Thus, corroborating with the use of DWI to differentiate OKC from OM.

According to Ogura et al. (2019)⁸, DWI may be useful in differentiating OKC and ameloblastomas, whereas it showed a minor contribution in differentiate cysts. Munhoz et al. (2019)¹⁷ found no statistical difference in the ADC values between dentigerous cyst (DC) and OKC, but found difference between ameloblastomas when compared to OKC and DC.

CONCLUSION

DWI can be useful as an auxiliary diagnostic tool in the process of differentiating OKC and other lesions, particularly ameloblastomas and odontogenic myxomas. Based on the difference in ADC values, it was possible to verify that the values concerning OKC were lower in the studies published so far, requiring a new prospective study to compare new cases with images acquired using the same MRI device and protocol.

REFERENCES

1. Borghesi A, Nardi C, Giannito C, Tironi A, Maroldi R, Bartolomeo FD, et al. Odontogenic Keratocyst: imaging features of a benign lesion with an aggressive behaviour. *Insights Imaging*. 2018;9(5):883-97.
2. Zachariades N, Papanicolaou S, Triantafyllou D. Odontogenic keratocysts: review of the literature and report of sixteen cases. *J Oral Maxillofac Surg*. 1985 Mar;43(3):177-82.
3. Sánchez-Burgos R, Gonzáles-Martín-Moro J, Pérez-Fernandez E, Burgueño-García M. Clinical, radiological and therapeutic features of keratocystic odontogenic tumours: a study over a decade. *J Clin Exp Dent*. 2014 Jul;6(3):e259-e64.
4. Caraca Ç, Dere KA, Er N, Aktas A, Tosun E, Köseoglu OT, et al. Recurrence rate of odontogenic keratocyst treated by enucleation and peripheral ostectomy: Retrospective case series with up to 12 years of follow-up. *Med Oral Patol Oral Cir Bucal*. 2018;23(4):e443-e8.
5. Gomes JPP, Costa ALF, Chone CT, Altemani AMAM, Altemani JMC, Lima CSP. Three-dimensional volumetric analysis of ghost cell odontogenic carcinoma using 3-D reconstruction software: a case report. *Oral Surg Oral Med Oral Pathol Oral Radiol*. 2017;123(5):e170-e5.
6. Gomes JPP, Veloso JRC, Altemani AMAM, Chone CT, Altemani JMC, Freitas CF, et al. Three-dimensional volume imaging to increase the accuracy of surgical management in a case of recurrent chordoma of the clivus. *Am J Case Rep*. 2018 Oct;19:1168-74.
7. Santos WP, Gomes JPP, Nussi AD, Altemani JM, Santos MTBR, Hasseus B, et al. Morphology, volume, and density characteristics of the parotid glands before and after chemoradiation therapy in patients with head and neck tumors. *Int J Dent*. 2020;2020:8176260.
8. Ogura I, Sasaki Y, Kameta A, Sue M, Oda T. Diffusion-weighted imaging in the oral and maxillofacial region: usefulness of apparent diffusion coefficient maps and maximum intensity projection for characterization of normal structures and lesions. *Pol J Radiol*. 2017;82:571-7.
9. Şerifoğlu I, Oz II, Damar M, Tokgoz O, Yazgan O, Erdem Z. Diffusion-weighted imaging in the head and neck region: usefulness of apparent diffusion coefficient values for characterization of lesions. *Diagn Interv Radiol*. 2015 May/ Jun;21(3):208-14.
10. Vanagundi R, Kumar J, Manchanda A, Mohanty S, Meher R. Diffusion-weighted magnetic resonance imaging in the characterization of odontogenic cysts and tumors. *Oral Surg Oral Med Oral Pathol Oral Radiol*. 2020 Oct;130(4):447-54.
11. Oda T, Sue M, Sasaki Y, Ogura I. Diffusion-weighted magnetic resonance imaging in oral and maxillofacial lesions: preliminary study on diagnostic ability of apparent diffusion coefficient maps. *Oral Radiol*. 2018 Sep;34(3):224-8.
12. Casseta M, Di Carlo S, Pranno N, Stagnitti A, Pompa V, Pompa G. The use of high resolution magnetic resonance on 3.0-T system in the diagnosis and surgical planning of intraosseous lesions of the jaws: preliminary results of a retrospective study. *Eur Rev Med Pharmacol Sci*. 2012 Dec;16(14):2021-8.
13. Sakamoto J, Kuribayashi A, Kotaki S, Fujikura M, Nakamura S, Kurabayashi T. Application of diffusion Kurtosis imaging to odontogenic lesions: Analysis of the cystic component. *J Magn Reson Imaging*. 2016 Dec;44(6):1565-71.
14. Srinivasan K, Bhalla AS, Sharma R, Kumar A, Choudhury AR, Bhutia O. Diffusion-weighted imaging in the evaluation of odontogenic cysts and tumours. *Br J Radiol*. 2012 Oct;85(1018):864-70.
15. Sumi M, Ichikawa Y, Katayama I, Tashiro S, Nakamura T. Diffusion-weighted MR imaging of ameloblastomas and keratocystic odontogenic tumors: differentiation by apparent diffusion coefficients of cystic lesions. *AJNR Am J Neuroradiol*. 2008 Nov;29(10):1897-901.
16. Han Y, Fan X, Su L, Wang Z. Diffusion-weighted MR imaging of unicystic odontogenic tumors for differentiation of unicystic ameloblastomas from keratocystic odontogenic tumors. *Korean J Radiol*. 2018 Jan/Feb;19(1):79-84.
17. Munhoz L, Nishimura DA, Hisatomi M, Yanagi Y, Asaumi J, Arita ES. Application of diffusion-weighted magnetic resonance imaging in the diagnosis of odontogenic lesions: a systematic review. *Oral Surg Oral Med Oral Pathol Oral Radiol*. 2012 Jul;130(1):85-100.
18. Neville B, Damm D, Allen CM, Chi AC. *Oral and maxillofacial pathology*. 4th ed. Amsterdam: Elsevier; 2016.